

Effect of Forewing and Hindwing Interactions on Aerodynamic Forces and Power in Hovering Dragonfly Flight

Z. Jane Wang* and David Russell†

Theoretical and Applied Mechanics, Cornell University, Ithaca, New York 14853, USA

(Received 13 December 2006; published 1 October 2007)

Dragonflies are four-winged insects that have the ability to control aerodynamic performance by modulating the phase lag (ϕ) between forewings and hindwings. We film the wing motion of a tethered dragonfly and compute the aerodynamic force and power as a function of the phase. We find that the out-of-phase motion as seen in steady hovering uses nearly minimal power to generate the required force to balance the weight, and the in-phase motion seen in takeoffs provides an additional force to accelerate. We explain the main hydrodynamic interaction that causes this phase dependence.

DOI: [10.1103/PhysRevLett.99.148101](https://doi.org/10.1103/PhysRevLett.99.148101)

PACS numbers: 47.63.-b, 47.32.C-, 47.32.Ff, 47.85.lb

A distinct feature of dragonfly flight is the phase relation between the forewings and hindwings during different maneuvers. Field and laboratory studies have found that during steady hovering the two sets of wings typically beat out of phase, and during takeoff the wings tend to beat nearly in phase [1–3]. The forewings and hindwings are about a chord length apart, close enough for them to interact hydrodynamically. It was speculated that the hydrodynamic interactions between forewings and hindwings might enhance the net vertical force compared to two independent wings [4,5], though recent 3D computations showed that the wing interaction reduces the net vertical force slightly when the two wings are not in phase [6]. What can be the advantage of counterstroking as observed during steady hovering? One advantage is that the alternating downstrokes reduce the force fluctuations and thus the body oscillation, which is desirable for hovering. Here we show that another advantage of counterstroking is minimizing the aerodynamic power.

There have been a number of experimental measurements of dragonfly in free and tethered flight [1–4,7]. To obtain the detailed wing kinematics sufficient for aerodynamic analysis, it is necessary to measure the time-dependent angle of attack in addition to wing velocities. For this, we filmed tethered dragonflies (*Libellula Pulchella*) to extract their 3D wing kinematics. The dragonflies were caught in fields and tested within 32 h of capture. A mirror was placed next to the insect so that the camera recorded pairs of mirror images to obtain 3D kinematics. The dragonfly was filmed at 1500 frames per second at the resolution of 512×1024 with a Phantom V5 high-speed camera. We used the deflection of the abdomen relative to the thorax as a cue to select flight sequences close to free flight. Specifically, we picked the cases where the longitudinal body aligns horizontally while the wings on two sides flap symmetrically, similar to those seen in the films of the free hovering dragonfly [2,4]. By tracking three painted points on each wing, we reconstructed the three-dimensional wing motions to deduce the time course of the

wing chord and the angle of attack. The 3D kinematics was then projected onto a cylindrical surface intersecting at $2/3$ of the span to form a 2D wing motion, which is an input to the computation.

Figure 1 shows the two-dimensional projection of a three-dimensional wing kinematics over a period. The gross features of the wing motion resemble those observed in previous experiments of free hovering [2,4], free forward [2], and ascending flight [3,7]. The wing flaps along a stroke plane which is tilted with respect to the longitudinal body. The mean flapping frequency is 33.4 Hz. The stroke plane angle (measured at the leading edge) is 53° for the forewing and 44° for the hindwing. These angles are similar to those reported in free ascending flight, 48° and 50° for the forewings and hindwings, respectively [3]. The up-and-down motion is asymmetric: the downstroke has a large angle of attack while the upstroke has a small angle of attack. When the stroke plane is inclined, the aerodynamic drag generated during the downstroke is oriented upward and makes a large contribution to the vertical force balance [8]. The hindwing leads the forewing by about 22° in temporal phase, based on the primary Fourier components. The Reynolds number $Re = \frac{c u_0}{\nu} = 4232$, where the chord $c = 1.03$ cm, the maximum velocity at $2/3$ span, $u_0 = 5.3$ m/s, and the kinematic viscosity of air, $\nu = 1.29 \times 10^{-5}$ m²/s.

To compute forces and power generated by the two wings, we solve the Navier-Stokes equation subject to multiple moving geometries. Our code [9] is formulated in terms of stream-vorticity functions on a uniform grid, which permits a fast solver using Fourier transform. A small overset grid is used in conjunction to track the interface of the wing. The wing geometry is a thin rectangle of an aspect ratio $1/16$ attached to two semicircular ends. The time integration is explicit and uses the 4th-order Runge-Kutta scheme. The numerical method has been tested against canonical examples of flow past cylinder and sinusoidal flapping motion [9]. Further details of experimental and computational methods were described in [9,10]. The

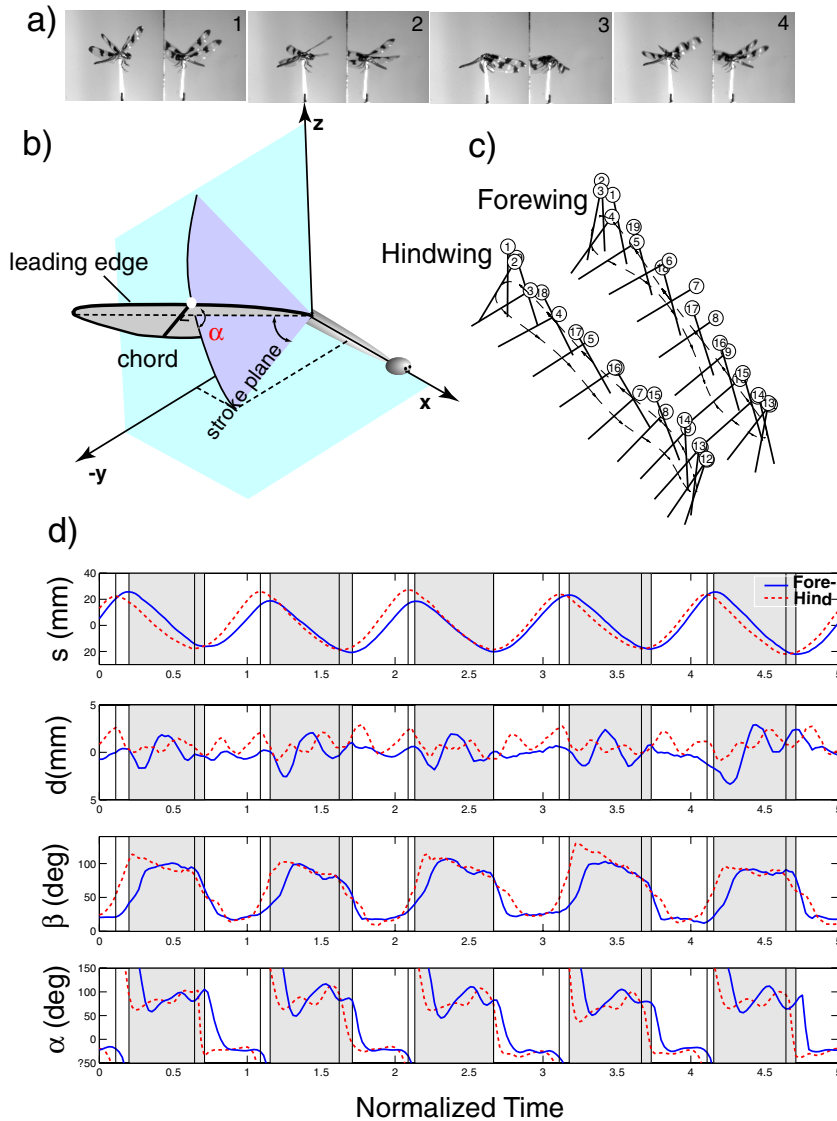


FIG. 1 (color online). Wing kinematics. (a) Pairs of mirror images of a tethered dragonfly during one period. (b) Schematics. (c) 2D projection of the chord positions of forewing and hindwing in one period. The leading edge is marked with a circle, and the number inside represents a time index. (d) Digitized data from film filtered to include the first 7 Fourier modes. s the distance along the stroke plane, d the distance out of the stroke plane, β the wing angle relative to the stroke plane, and α is the wing angle of attack, defined as the angle between the chord and the wing velocity. Shaded regions indicate forewing downstroke, and vertical lines indicate stroke reversal.

2D approximation is chosen for simplicity. The similarity and difference between 2D and 3D forces on a hovering dragonfly wing was described in [11]. Here we compare the 2D aerodynamic forces and power among different wing motions. Throughout the Letter, the force and power refer to the sum of the force and power on the forewings and hindwings.

Computing unsteady flows at $Re \sim O(10^3)$ subject to moving geometries with sharp tips is expensive. To examine the Reynolds number dependence of the flows and forces, we compare two cases, $Re = 200$ and 1000 , shown in Fig. 2. The vorticity field is more complex than those seen in single-wing computations [12], but on average, the wing motion creates a downward flow and thus an upward net force on the wings. The detailed vortex structures at the two Reynolds numbers are markedly different, with apparent finer structures at higher Reynolds number as expected. However, the forces in the two cases are qualitatively similar, with the averaged force slightly higher in the high Reynolds number. In both cases, the flows are highly

separated due to the high angle of attack during downstroke, and the associated pressure force is relatively insensitive to the Reynolds number. This is analogous to flow past a cylinder in the separated flow regime, where the drag coefficient is fairly constant in $Re \sim (10^2, 3 \times 10^5)$ [13]. We also note that $Re = 200$ is an order of magnitude higher than the transitional Reynolds number, of $O(10)$, above which the locomotion is dominated by fluid inertia [14–16]. We take advantage of these facts to compute forces and power at the lower Reynolds number $Re = 200$, which allows us to explore the effects of phase dependence with less computing time.

The phase dependence of the averaged vertical force (F_y) and power (P) is shown in Fig. 3. Because the wings move along an inclined stroke plane, we do not expect symmetry between $\phi \in [0^\circ, 180^\circ]$ (the hindwing leads) and $\phi \in [180^\circ, 360^\circ]$ (the forewing leads). The force and power can vary about 60% and 40%, respectively, due to the phase variation. The maximal force and power occur at $\phi = 0^\circ$, and the minimal force and power occur at

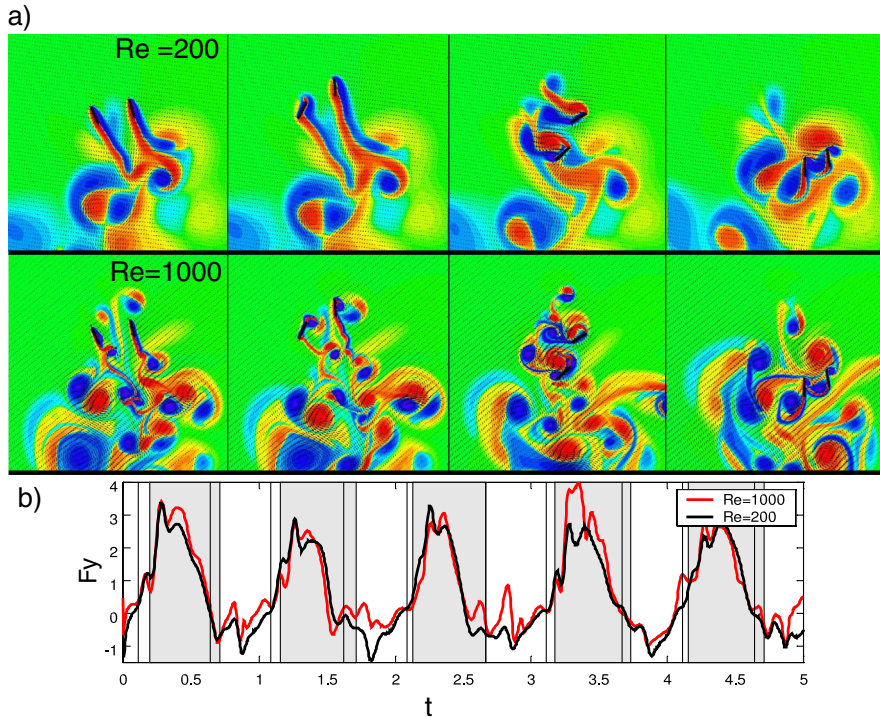


FIG. 2 (color online). Comparison of flows and forces at $Re = 200$ and $Re = 1000$. (a) Nondimensional vorticity field (ω) at four different times during one period. Color value = $\text{sign}(\omega) \log(1.0 + |\omega|)$, and is plotted on a scale of $-8:2/3:8$, with red for positive vorticity, blue negative vorticity. (b) Nondimensional vertical force obtained as follows: the 2D computed force is extrapolated to 3D using the blade-element assumption, and the 3D force is divided by the weight of the insect. The plotted F_y is the projection of the 3D force in the vertical direction.

$\phi \sim 40^\circ$ and $\phi \sim 160^\circ$, respectively. For $\phi < 100^\circ$, the force and power depend sensitively on ϕ , whereas for $\phi \in [100^\circ, 220^\circ]$ the force and power stay roughly constant, varying about $\pm 5\%$ and 5% , respectively (see gray box in Fig. 3). The force drops substantially when $\phi \in [40^\circ, 80^\circ]$. For steady hovering, the net force must balance the weight, and hovering with $\phi \in [100^\circ, 220^\circ]$ seems to have two benefits. First, it can reduce the power in generating the required force, and second, the control of the phase needs not be exact. For takeoffs, the net force must exceed the weight in order to accelerate. The in-phase motion can increase the force by about 40% compared to the out-of-phase motion, and thus can be used for accelerating flight at an expected higher cost.

The above results are obtained for a specific family of wing motions and our computations are in 2D. To understand whether these limitations will affect the qualitative results obtained here, it is instructive to have an explanation of the main hydrodynamic effect due to wing interactions. The wing-wing interactions were previously studied for several different wing kinematics. For instance, the effect of the phase on the propulsion efficiency of two wings undergoing symmetrical heaving and pitching motions in forward flight was calculated using a quasi-vortex-lattice model [17]. The theory, by construction, calculates the aerodynamic lift and leading edge suction force on each wing, and its results may be applicable to the recent experiments of two vertically stacked wings undergoing similar wing motions in rotated coordinates [18]. The theory, however, does not take into account the aerodynamic drag due to flow separation that constitutes much of the force generated by the hovering motion studied here.

Recent related computation of forward flight of dragonflies examined the forces, though not power, and noted that the presence of a second wing reduces the averaged force slightly due to the downwash effect [6]. This downwash is an averaged flow effect which is expected to occur also in 2D flows; however, it would not explain the explicit phase dependence seen in Fig. 3 which must depend on the instantaneous flow.

A visual inspection of instantaneous flows provided little insight into the effect of the phase on the net force and

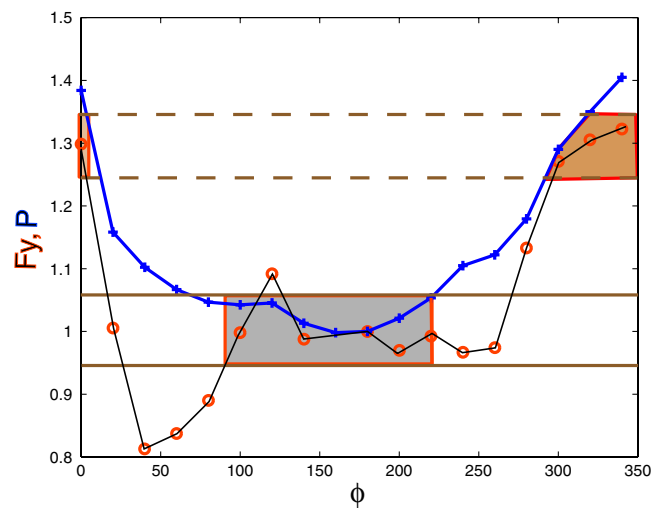


FIG. 3 (color online). Time averaged vertical force, F_y (circles), and power P (pluses), as a function of phase (ϕ). The force and power are normalized with their respective values at $\phi = 180^\circ$.

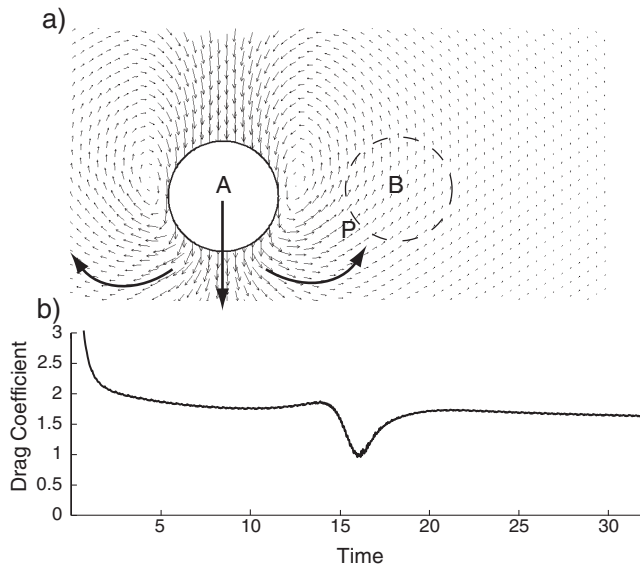


FIG. 4. The effect of the induced flow. (a) Vectors represent the induced flow due a downward moving cylinder *A*. The induced flow is upward near the location of the second cylinder *B*. Thus, *B* will experience an increased drag if it moves downward and a reduced drag if moves upward. The motion of *B* has a similar effect on *A*. (b) the time-dependent drag coefficient on one of the two cylinders moving in opposite directions, separated by a distance of 1.5 radii [9]. The drag is reduced as the two cylinders pass each other, and the drag is minimal at $t = 16$ (in computational unit) when the two cylinders are in the closet proximity.

power. The vortices in these cases can indicate the general direction of the force, but are insufficient to reveal the subtle change in the magnitude of the force. This is because it is difficult to sum up the momentum of all the vortices based on the visual image. Instead, we consider the analogous case of two cylinders moving in parallel next to each other. Previously we noticed that the drag on each cylinder is reduced if the two cylinders move in opposite directions [9]. This effect on the drag can be partially explained in Fig. 4. If both cylinders move in the same direction, each cylinder will encounter a larger effective flow, which is the superposition of its own velocity and the induced flow due to the other cylinder. The larger incoming velocity results in a larger drag on the cylinder. On the other hand, if the cylinders move in opposite directions, the drag on each cylinder is reduced due to the reduced effective incoming flow. Figure 4 shows the time history of the drag coefficient on one of the two cylinders approaching each other. The drag drops almost by a factor of 2 as they pass each other in the closest proximity. Returning to the hovering dragonfly, when the two wings move in phase, the increase in drag on

both wings point to the same direction. Thus the in-phase stroke generates a larger net force, accompanied by a larger power. When the two wings move out of phase, the reduction in drag on the two wings point to opposite directions, this leads to an insignificant change in the net force. However, the power reduction adds so that the net power is reduced. In other words, the counterstroking provides a mechanism for generating nearly the same drag force while reducing the power. Last, the power reduction is most pronounced if the two wings meet near the midstroke, where the wing velocity is maximal. This happens when the two wings move at a phase near 180° .

We are grateful to Jim Marden at Penn State University for his generous help with the dragonfly experiment. We thank Attila Bergou for double checking some of the force calculations using a different computational method. The work is supported by NSF, AFOSR, and Packard Foundations.

*Corresponding author.
zw24@cornell.edu

†Permanent address: Itasca Consulting Group, Inc., Minneapolis, MN 55401, USA.

- [1] D. E. Alexander, *J. Exp. Biol.* **109**, 379 (1984).
- [2] G. Ruppell, *J. Exp. Biol.*, **144**, 13 (1989).
- [3] J. M. Wakeling and C. P. Ellington, *J. Exp. Biol.* **200**, 557 (1997).
- [4] R. A. Norberg, *In Swimming and Flying in Nature*, edited by T. Y. Wu, C. J. Brokaw, and C. Brennen (Plenum Press, New York, 1975), Vol. 2, pp. 763–780.
- [5] C. Soms and M. W. Luttges, *Science* **228**, 1326 (1985).
- [6] J. K. Wang and M. Sun, *J. Exp. Biol.* **208**, 3785 (2005).
- [7] H. Wang, L. Zeng, H. Liu, and C. Yin, *J. Exp. Biol.* **206**, 745 (2003).
- [8] Z. J. Wang, *J. Exp. Biol.* **207**, 4147 (2004).
- [9] D. Russell and Z. J. Wang, *J. Comput. Phys.* **191**, 177 (2003).
- [10] D. Russell, Ph.D. dissertation, Cornell University, 2004.
- [11] M. Sun and S. Lan, *J. Exp. Biol.* **207**, 1887, 2004.
- [12] Z. J. Wang, *Phys. Rev. Lett.* **85**, 2216, 2000.
- [13] D. J. Tritton, *Physical Fluid Dynamics* (Oxford Science Publications, Oxford, 1988).
- [14] S. Childress and R. Dudley, *J. Fluid Mech.* **498**, 257 (2004).
- [15] L. Miller and C. Peskin, *J. Exp. Biol.* **207**, 3073 (2004).
- [16] S. Alben and M. Shelley, *Proc. Natl. Acad. Sci. U.S.A.* **102**, 11 163 (2005).
- [17] C. E. Lan, *J. Fluid Mech.* **93**, 747 (1979).
- [18] W. J. Maybury and F. O. Lehmann, *J. Exp. Biol.* **207**, 4707 (2004).